# MICROWAVE ABSORPTION PERFORMANCES OF COPPER/NICKEL FERRITE@FIBER POLYANILINE

**Tran Quang Dat*, Nguyen Tran Ha, Nguyen Vu Tung, Pham Van Thin**

*Le Quy Don Technical University*

**Abstract**

In this work, we present the recent study in the microwave absorption performances of the $Cu_{0.5}Ni_{0.5}Fe_2O_4$@polyaniline (CNF@PANI). This material has been synthesized by polymerization and hydrothermal reaction process. The PANI fiber structure with the whole cover of CNF nanoparticles could establish the improvement of microwave absorption performances. The value of optimal reflection loss reached -60.9 dB at 12.9 GHz with the sample which had thicknesses of 2.5 mm and the widest effective bandwidth is up to 6.1 GHz with the sample which had thicknesses of 2.0 mm. By varying the thickness within the range of 2.0 to 3.5 mm, this effective bandwidth will cover the entire X and Ku bands.

***Keywords:*** *$Cu_{0.5}Ni_{0.5}Fe_2O_4$; PANI; fiber; microwave absorption.*

## 1. Introduction

Currently, low thickness, lightweight, cost-effectiveness, and a wide bandwidth are all desirable characteristics of an ideal absorber [1]. Pure dielectric or magnetic materials are insufficient for effective radiation absorption [2]. Many advanced experiments have been carried out in recent years in order to produce new magnetic nanomaterials with complex chemical and magnetic properties [3]. Due to the advantages of inorganic and organic materials, conducting polymers have arisen as significant groups of polymers with numerous applications in the fields of optical, photonic, and electrical properties [4]. Polyaniline is a promising conductive polymer which is widely used as microwave absorbing materials because of its good environmental stability, electrochemical behavior, and customizable electromagnetic parameters [5]. However, pure PANI microwave absorption properties are mostly due to dielectric loss, which is inadequate for long-range use. Spinel ferrites have been commonly used as microwave absorbers due to their good chemical stability, high saturation magnetization and high magnetic loss. On the other hand, spinel ferrites are limited in their applications due to their high density and short absorption bandwidth, as well as a single magnetic loss mechanism [3]. The hybrid material combines the magnetic loss properties of ferrite with the dielectric loss properties of conductive polymers, allowing the absorber's microwave absorption properties to be greatly

* Email: dattq@lqdtu.edu.vn

improved. Furthermore, producing nanostructures with complex morphologies is a reliable method for improving microwave absorption performance while reducing material loading [6].

In previous our reports, CNF@PANI materials have been prepared by the polymerization and hydrothermal reaction and process [7]. The purpose of this study is to investigate the feasibility of microwave absorption of CNF@PANI. The CNF@PANI exhibits wide effective absorption bandwidth and strong microwave absorption performance in paraffin with a low mass filling ratio (30 wt%).

## 2. Experimental

First, polyaniline fiber was synthesized by polymerization reaction. Second, coprecipitation and hydrothermal treatment methods were used to produce $Cu_{0.5}Ni_{0.5}Fe_2O_4$@PANI [7].

In a typical experiment, the homogeneous mixture was prepared by mixing the CNF@PANI material and paraffin wax. The substance in the mixture accounted for 30% of the total weight. The final compounds were pressed into a toroidal form with a 3.04 mm inner diameter and a 7.0 mm outer diameter. The microwave absorption properties were measured by utilizing Keysight PNA-X N5242A vector network analyzer. The microwave absorption properties were determined using the transmission line principle [8]. The reflection loss (RL) was measured using the following equations in detail:

$$RL(dB) = 20.\log\left|\frac{Z_{in}-1}{Z_{in}+1}\right| \tag{1}$$

$$Z_{in} = \sqrt{\frac{\mu_r}{\varepsilon_r}}\tanh\left(j\frac{2\pi fd}{c}\sqrt{\mu_r\varepsilon_r}\right) \tag{2}$$

where $Z_{in}$ is the input impedance of the absorber, $\varepsilon_r$ and $\mu_r$ is the complex relative permitivity and permeability respectively, $c$ is the velocity of electromagnetic waves in vacuum, $f$ is the frequency of electromagnetic wave, and $d$ is the thickness of samples.

## 3. Results and discussion

### *3.1. Morphology and structure characterization of material*

The morphologies of the PANI material were observed by SEM and shown in Fig. 1(a). Actually, the fibers are completely homogenous. The value of the diameter of the fibers is about 100 nm. The frame of PANI which was also shown with long fibers and their interconnection. The PANI frame is likely to generate multiple interfaces, which is beneficial for interfacial polarization and electromagnetic wave attenuation.

Fig. 1(b) presents the SEM image of CNF@PANI material. The small nanoparticles, which have a diameter of 10-15 nm was wholly covered onto the surface of PANI.

Fig. 2 presents the FT-IR spectra of CNF@PANI material. The peak at 563 $cm^{-1}$ is related to the stretching vibrations of Fe-O bonds. The peaks at 832, 1167, 1305 $cm^{-1}$ could be ascribed to the vibrations of C-H, C-O and C-N bondings, respectively. The vibrations of C=C stretching of quinonoid and benzenoid rings are associated to the absorption peaks at 1592 and 1496 $cm^{-1}$ [9].

In the XRD pattern of CNF@PANI sample (Fig. 3), the characteristic peaks for (hkl) planes such as (111), (220), (311), (222), (400), (422), (511) and (440) were observed at 18.1º, 30.0º, 35.3º, 36.9º, 42.9º, 53.6º, 56.9º and 62.3º, respectively. The XRD data indicated that the CNF particles have the face-centered cubic trevorite structure [5]. The peaks of PANI vanished in XRD pattern because the CNF nanoparticles interfere with PANI fiber.

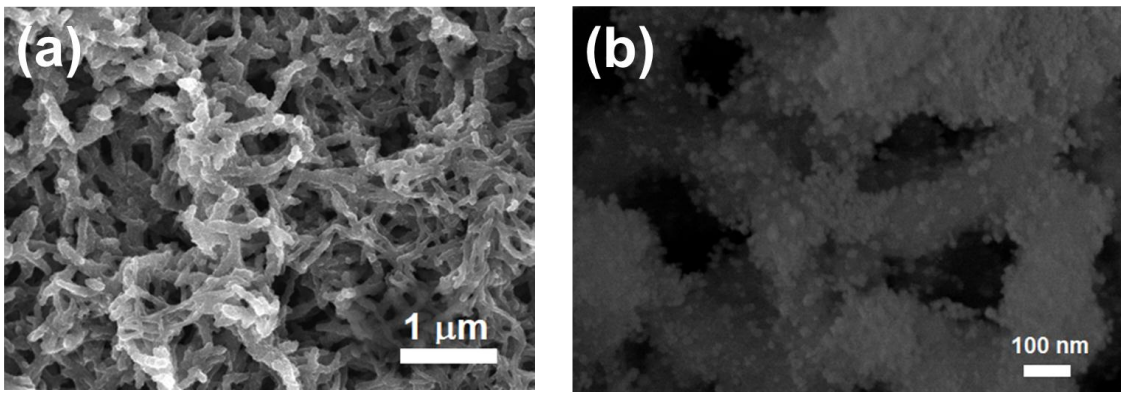


*Fig. 1. SEM images of (a) PANI and (b) CNF@PANI.*

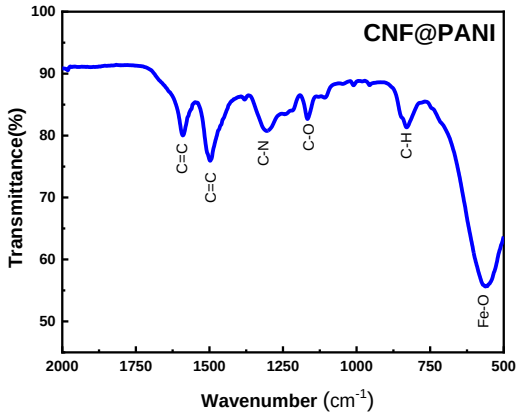


*Fig. 2. FT-IR spectra of CNF@PANI.*

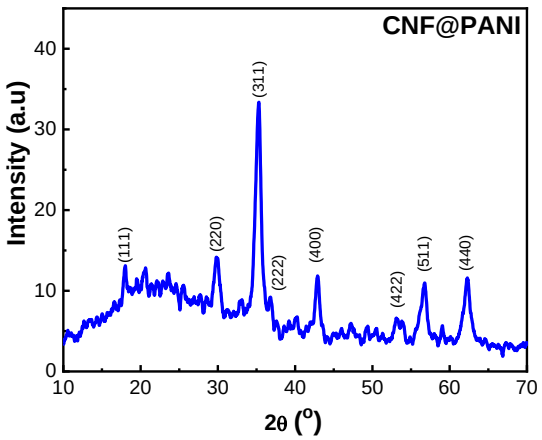


*Fig. 3. XRD patterns of CNF@PANI.*

### *3.2. Microwave absorption properties of material*

The frequency dependency curves of real and imaginary complex permittivity and permeability of a sample with a thickness of 2.5 mm are shown in Fig. 4. As can be shown in this figure, the values of the real part of relative complex permittivity ($\varepsilon'$) are in the range of 10.6 ÷ 15.1 and the range of values of the imaginary part ($\varepsilon''$) of relative complex permittivity is 4.3 ÷ 6.5. The real and imaginary parts of relative complex permittivity consistently show a decreasing trend with frequency. The high values of $\varepsilon'$ of CNF@PANI hybrid indicate that the CNF nanoparticles implanted on PANI fiber and the resulting hetero-structure significantly improve the dielectric properties of this material. It was also approved for the enhancement of dipolar and interfacial polarization, as well as low resistivity, which contributed to the materials' effective electronic transmission proficiency [10].

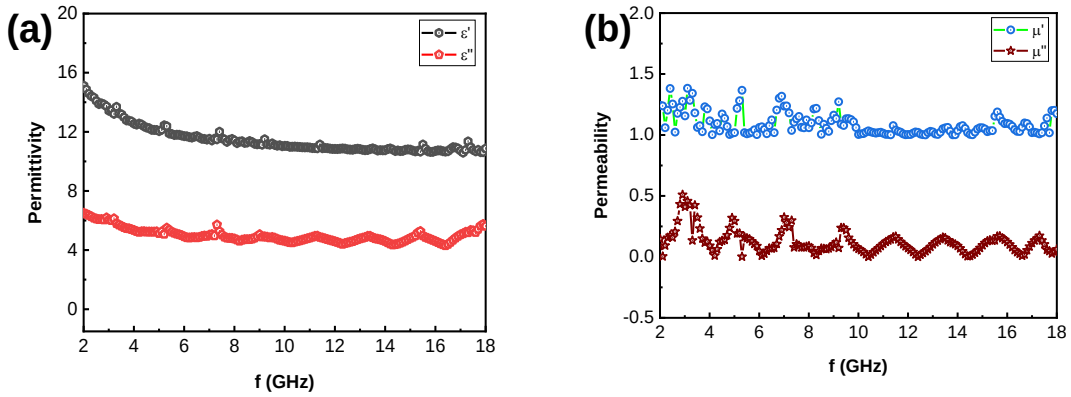


*Fig. 4. The real, imaginary part of (a) complex permittivity and (b) complex permeability of CNF@PANI material.*

Additionally, in the frequency range of 2 ÷ 18 GHz, significant resonance peaks of imaginary part ($\mu''$) can be found. The values of $\mu''$ are greater than zero means that the CNF@PANI material has a significant magnetic loss, which is mostly due to natural resonance and exchange resonance. As seen in this figure, the values of real part ($\mu'$) generally present sudden peaks or so, other remain a constant at 1.

On the basis of Debye relaxation theory [11], the dielectric properties of the material are further examined by the association between real part and imaginary part of complex permittivity. One relaxing mechanism can be carried out using the Cole-Cole equation as follows:

$$\left(\varepsilon' - \frac{\varepsilon_s + \varepsilon_\infty}{2}\right)^2 + \left(\varepsilon''\right)^2 = \left(\frac{\varepsilon_s - \varepsilon_\infty}{2}\right)^2 \quad (3)$$

where $\varepsilon_s$, $\varepsilon_\infty$ are the static permittivity and the relative permittivity at the high-frequency limit.

The plot of $\varepsilon'$ versus $\varepsilon''$ would be displayed whole semicircle which corresponds to a Debye relaxation process. As shown in Fig. 5, multiple distinct semicircles can be noticeably observed, which indicates that the multi-dielectric relaxation process occurs in the composite material. Furthermore, the distorted Cole-Cole semicircles indicate the presence of dielectric loss-enhancing mechanisms such as defect polarization, interfacial polarization, and conductive loss [12]. Under the external electromagnetic field, the heterogeneous interfaces in CNF@PANI may produce further polarization centers, increasing interfacial polarization and improving relevant relaxation.

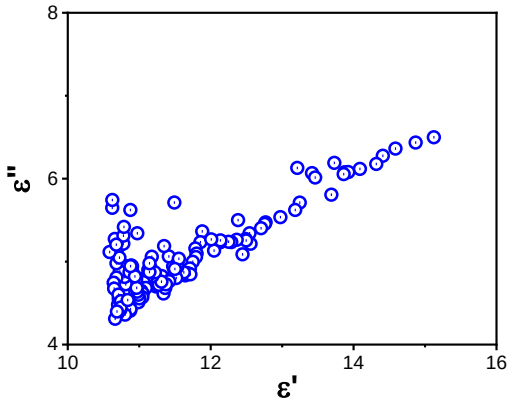


*Fig. 5. The typical Cole-semicircle curve of CNF@PANI.*

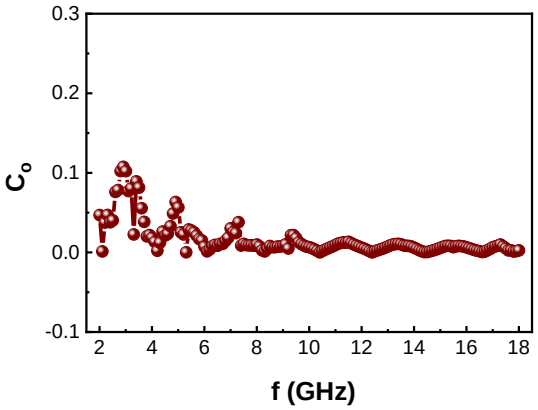


*Fig. 6. The $C_0$ - $f$ values of CNF@PANI.*

Commonly, in the frequency range 2 ÷ 18 GHz, eddy current loss is also a significant contributor to magnetic loss which can be estimated by the coefficient $C_0$ defined as $C_0 = \mu''/(\mu'^2.f)$, where $f$ is frequency. As seen from the Fig. 6, the value of $C_0$ changes slightly in the 8 ÷ 18 GHz, which suggests that the magnetic loss is mainly caused by the eddy current effect. The natural resonance effect causes magnetic loss in the 2 ÷ 8 GHz band due to the presence of resonance peaks.

The impedance matching, as far as we know, refers to the tendency of incident electromagnetic waves to enter the interior of the material in order to minimize direct reflection of electromagnetic waves. The absorption properties of material would be stronger if the $Z_{in}$ is close to 1. From Fig. 7, the value of impedance matching of CNF@PANI sample with the thickness of 2.5 mm is closest to 1 at 12.9 GHz. It suggests that incident electromagnetic waves could penetrate CNF@PANI hybrid efficiently and be absorbed effectively.

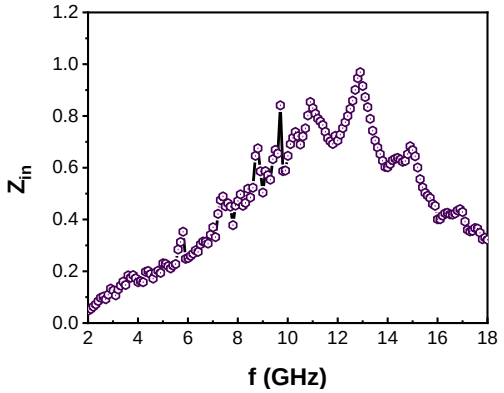


*Fig. 7. The impedance matching of CNF@PANI sample at 2.5 mm.*

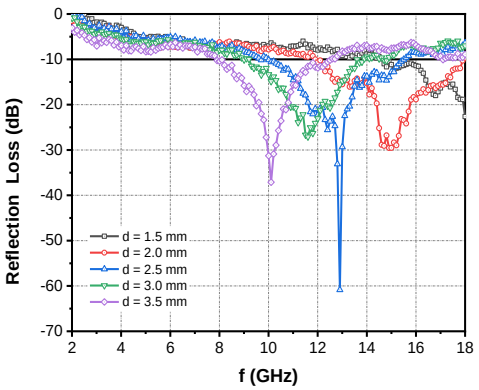


*Fig. 8. Reflection loss of CNF@PANI samples.*

The microwave reflection loss (RL) at different thickness is depicted in Fig. 8. With rising thickness, the RL curve gradually changes to lower frequency. The phenomenon is explained by the matching relationship between frequency and the matching thickness $d_m$ of the absorption materials [13]:

$$d_m = \frac{k.c}{4f\sqrt{|\varepsilon_r|.|\mu_r|}} \qquad k = 1,3,5... \tag{4}$$

By varying the frequency and thickness of the absorbing material, optimum matching and absorption could be achieved. The effective absorption bandwidth (RL ≤ -10 dB) of samples are 6.1, 5.5, 4.9 and 4.6 GHz with the thickness of 2.0, 2.5, 3.0 and 3.5 mm, respectively. It is obvious that with increasing absorber thickness the absorption bandwidth gradually narrows. The best effective absorption bandwidth which is 6.1 GHz (11.9 ÷ 18.0 GHz) exhibited at the thickness of 2.0 mm. Furthermore, the effective absorption bandwidth in both the X and Ku bands (8.0 ÷ 18.0 GHz) can be achieved by changing the thickness of the CNF@PANI material. What's more, the best minimum reflection loss of CNF@PANI is -60.9 dB at the frequency 12.9 GHz with a small thickness of 2.5 mm.

The microwave absorption properties of ferrite-PANI composite materials are compared in Table 1. According to these findings, CNF@PANI material has particularly strong microwave absorption properties, including high reflection loss, effectively broad absorption bandwidth, and a thin thickness.

The remarkable microwave absorption performance of the CNF@PANI material is correlated to its structure original and composition. Firstly, the abundant oxygen vacancies and significant lattice defects in the porous composite will behave as dipoles in the alternating electromagnetic field, causing a strong dipole polarization effect [10]. Secondly,

the electromagnetic wave dissipation is aided by the unique multi-channel pore in the fiber-like and network of CNF@PANI material [8]. Thirdly, the PANI fibers anchored by CNF nanoparticles, not only prevent them from stacking together, but also may penetrate and increase multiple reflection and scattering in between pieces of the inner space of the structure [6]. Finally, the combination of dielectric and magnetic loss produces in excellent impedance matching and improved electromagnetic wave absorption efficiency.

*Table 1. Comparison of the microwave absorption properties with other absorbers.*

| **Absorber** | **$RL_{min}$ (dB)** | **Bandwidth (GHz) (RL ≤ -10 dB)** | **Thickness (mm) Filled ratio (wt%)** | **Ref.** |
|---|---|---|---|---|
| PANI@$BaFe_{12}O_{19}$ | -17.4 | 2.4 | 4.5 (80%) | [14] |
| PANI@$CoFe_2O_4$ | -28.4 | 0.3 | 4.0 (50%) | [15] |
| PANI@MnNiZn | -31.3 | 3.7 | 3.0 (25%) | [16] |
| PANI@NiZnNd | -37.4 | 4.9 | 4.0 (70%) | [8] |
| PANI@NiZn | -39.6 | 3.0 | 2.5 (25%) | [10] |
| NiZn/$BaFe_{12}O_{19}$@PANI | -25.6 | 7.2 | 3.5 (60%) | [6] |
| **$Cu_{0.5}Ni_{0.5}Fe_2O_4$@PANI** | **-60.9** | **6.1** | 2.5 (30%)<br>2.0 (30%) | This work |

## 4. Conclusion

In summary, the structure of composite material which has CNF nanoparticles uniformly anchored on the surface of PANI fibers exhibited a significant microwave absorption performance. The electromagnetic wave absorption performance of the CNF@PANI hybrid is due to its hierarchical porous structure, synergistic effect of dielectric and magnetic loss, and impedance matching. The optimal value of reflection loss of -60.9 dB was obtained at 12.9 GHz with the sample which had thicknesses of 2.5 mm. The maximum effective bandwidth reached 6.1 GHz (11.9 ÷ 18 GHz) at a thickness of 2.0 mm, which completely covered the entire Ku band (12 ÷ 18 GHz). By varying the thickness between 2.0 and 3.5 mm, this effective bandwidth will cover the whole 8 ÷ 18 GHz bands. Therefore, the CNF@PANI material prepared herein would have a good application prospect for the effective absorption of X - Ku bands.

## Acknowledgements

The investigation was supported by Le Quy Don Technical University under the grant No. 20.DH.03.

## References

[1] M. Green, X. Chen, "Recent progress of nanomaterials for microwave absorption," *Journal of Materiomics*, 5(4), 503-541, 2019.

[2] F. Meng, H. Wang, F. Huang, Y. Guo, Z. Wang, D. Hui and Z. Zhou, "Graphene-based microwave absorbing composites: A review and prospective," *Compo. B. Eng.*, 137, 260-277, 2018.

[3] A. Houbi, Z.A. Aldashevich, Y. Atassi, Z. B. Telmanovna, M. Saule, K. Kubanych, "Microwave absorbing properties of ferrites and their composites: A review," *J. Magn. Magn. Mater.*, 529, 167839, 2021.

[4] F. Kazemi, S.M. Naghi, Z. Mohammadpour, "Multifunctional micro-/nanoscaled structures based on polyaniline: An overview of modern emerging devices," *Mater. Today Chem.*, 16, 100249, 2020.

[5] T.Q. Dat, N.T. Ha and D.Q. Hung, "Reduced Graphene Oxide - $Cu_{0.5}Ni_{0.5}Fe_2O_4$ - Polyaniline Nanocomposite: Preparation, Characterization and Microwave Absorption Properties," *J. Electron. Mater.*, 46 (6, 3707-3713), 2017.

[6] X. Meng, Q. Han, Y. Sun, Y. Liu, "Synthesis and microwave absorption properties of $Ni_{0.5}Zn_{0.5}Fe_2O_4$/$BaFe_{12}O_{19}$@polyaniline composite," *Ceram. Int.*, 45, 2504-2508, 2019.

[7] T.Q. Dat, N.V. Tung, P.V. Thin, "Porous polyaniline - copper/nickel ferrite composite for enhanced adsorption of uranium from aqueous," *Vietnam National Conference on Solid state Physics and Materials Science*, 11, 107-113, 2019.

[8] Z. Jiao, Z. Yao, J. Zhou, K. Qian, Y. Lei, B. Wei, W. Chen, "Enhanced microwave absorption properties of Nd-doped NiZn ferrite/ polyaniline nanocomposites," *Ceram. Int.*, 46, 25405-25414, 2020.

[9] H. Jia, H. Xing, X. Ji, S. Gao, "Self-template and in-situ polymerization strategy to lightweight hollow $MnO_2$@polyaniline core-shell heterojunction with excellent microwave absorption properties," *Appl. Surf. Sci.*, 537, 147857, 2021.

[10] N.N. Ali, Y. Atassi, A. Salloum, A. Charba, A. Malki, M. Jafarian, "Comparative study of microwave absorption characteristics of (Polyaniline/NiZn ferrite) nanocomposites with different ferrite percentages," *Mater. Chem. Phys.*, 211, 79-87, 2018.

[11] X. Wang, T. Zhu, S. Chang, Y. Lu, W. Mi and W. Wang, "3D Nest-like architecture of core-shell $CoFe_2O_4$@1T/2H-$MoS_2$ composites with tunable microwave absorption performance," *ACS Appl. Mater. Interfaces.*, 12(9, 11252-11264), 2020.

[12] K. Zhang, J. Luo, N. Yu, M. Gu, X. Sun," Synthesis and excellent electromagnetic absorption properties of reduced graphene oxide/PANI/$BaNd_{0.2}Sm_{0.2}Fe_{11.6}O_{19}$ nanocomposites," *J. Alloys. Compd.*, 779, 270-279, 2019.

[13] X. Su, J. Wang, X. Zhang, S. Huo, W. Chen, W. Dai, B. Zhang, "Design of controlled-morphology $NiCo_2O_4$ with tunable and excellent microwave absorption performance," *Ceram. Int.*, 46 (6), 7833-7841, 2020.

[14] W.J. Feng, X. Zhao, W.Q. Zheng, "Microwave absorption properties of $BaFe_{12}O_{19}$ prepared in different temperature with Polyaniline nanocomposites," *Adv. Mater. Res.*, 1142, 211-215, 2017.

[15] M.M. Ismail, S.N. Rafeeq, J.M.A. Sulaiman, A. Mandal, "Electromagnetic interference shielding and microwave absorption properties of cobalt ferrite $CoFe_2O_4$/polyaniline composite," *Appl. Phys. A.*, 124, 380-391, 2018.

[16] N.N. Ali, B.A.R. Al-Qassar, Y. Atassi, A. Salloum, A. Malki, M. Jafarian, "Design of lightweight broadband microwave absorbers in the X-band based on (polyaniline/MnNiZn ferrite) nanocomposites," *J. Magn. Magn. Mater.*, 453, 53-61, 2018.

# TÍNH CHẤT HẤP THỤ VI SÓNG CỦA VẬT LIỆU $Cu_{0.5}Ni_{0.5}Fe_2O_4$@ SỢI PANI

***Tóm tắt:*** *Trong nghiên cứu này, chúng tôi trình bày các nghiên cứu về đặc tính hấp thụ vi sóng của vật liệu $Cu_{0.5}Ni_{0.5}Fe_2O_4$@polyanilin (CNF@PANI). Vật liệu được tổng hợp từ các quá trình phản ứng polymer hóa và thủy nhiệt. Cấu trúc sợi PANI được phủ bởi các hạt nano CNF trên bề mặt tạo nên sự cải thiện của các đặc tính hấp thụ vi sóng. Giá trị tổn hao phản xạ đạt được là -60,9 dB tại tần số 12,9 GHz với mẫu có bề dày 2,5 mm và dải băng hấp thụ hiệu quả lên tới 6,1 GHz ứng với mẫu có bề dày 2,0 mm. Bằng cách điều chỉnh bề dày từ 2,0 đến 3,5 mm, dải tần số hấp thụ hiệu quả có thể bao phủ toàn bộ dải băng X và Ku.*

**Từ khóa:** $Cu_{0.5}Ni_{0.5}Fe_2O_4$; PANI; sợi; hấp thụ vi sóng.

*Received:* 05/04/2020; *Revised:* 27/07/2021; *Accepted for publication:* 02/08/2021

❑